Phonon analogue of topological nodal semimetals

Hoi Chun Po, Yasaman Bahri, and Ashvin Vishwanath
Department of Physics, University of California, Berkeley, California 94720, USA
(Dated: October 7, 2014)

Recently, Kane and Lubensky proposed a mapping between bosonic phonon problems on isostatic lattices to chiral fermion systems based on factorization of the dynamical matrix [Nat. Phys. **10**, 39 (2014)]. The existence of topologically protected zero modes in such mechanical problems is related to their presence in the fermionic system and is dictated by a local index theorem. Here we adopt the proposed mapping to construct a two-dimensional mechanical analogue of a fermionic topological nodal semimetal that hosts a robust bulk node in its linearized phonon spectrum. Such topologically protected soft modes with tunable wavevector may be useful in designing mechanical structures with fault-tolerant properties.

arXiv:1410.1320v1 [cond-mat.mes-hall] 6 Oct 2014

Correspondences between bosonic and fermionic problems have long been an indispensable tool for both solving and understanding model systems. Conventional mappings like the Jordan-Wigner transformation and bosonization, however, are generally exact, with a few known exceptions, only in one spatial dimension [1, 2]. For free particles, both bosonic and fermionic Hamiltonians are characterized by a quadratic form defined by a representation matrix, and the statistics of the particles are reflected in the different algebras invoked in canonical transformations [3] and the positive semi-definiteness of the representation matrix for a stable bosonic system [4, 5]. Despite such differences, one can nonetheless establish an equivalence between the spectra of a bosonic and a fermionic problem by factoring the corresponding representation matrices [4–6]. Although this approach is limited to free or weakly interacting particles, unlike most other mappings, it is both independent of dimensionality and is itself a local mapping. It is therefore of interest to explore the extent to which this correspondence can provide a new perspective.

The recent realization of the existence of surface modes dictated by topological properties of the bulk has generated immense interest across the community [6–12]. Topological insulators, for instance, are electronic systems that host protected conducting surface states but are insulating in their bulk [7]. Within the free fermion description, the existence of these robust surface states can be predicted, via the bulk-boundary correspondence, by computing the topological invariants associated with the occupied Bloch bands [7]. More recently, certain mechanical (mass-spring) problems were independently found to host robust zero-energy modes localized at boundaries [13]. The boson-fermion mapping proposed by Kane and Lubensky demonstrates that these phenomena are related [6]: the boundary phonon modes found in certain isostatic lattices can be understood as a manifestation of the topological properties of a chiral fermion problem.

An interesting open problem is to ask if phonon analogues can be found for systems which lie beyond the context considered in [6]. For instance, the mapping [6] was formulated for mechanical structures with a frame description, for which the Hamiltonian can be defined in terms of the set of spring extensions. Restricting to such models, any phonon problem has a well-defined fermionic counterpart. The extent to which this holds for mechanical problems outside of the frame description is an open question. Furthermore, Ref. [6] considered localized boundary modes assuming a gapped bulk; a similar setting can also give rise to phonon zero modes localized around defects [12]. In contrast, one may search for phonon analogues of fermionic systems with a gapless node in the bulk protected by non-trivial band topology, as opposed to symmetry which protects phonons originating via Goldstone's theorem. This is the problem considered in this work.

Topological nodal semimetals (TNS) have topologically protected bulk zero modes and unusual surface states [8, 9, 14]. The Weyl semimetal, one such TNS, is characterized by the touching of nondegenerate Bloch bands at isolated points or lines in momentum space (Fig. 1). Although Weyl points are generic in 3D, they have codimension 2 in 2D and are not generic unless a symmetry is present [8, 9, 14]. A Weyl node has an associated chirality originating from a discontinuity in a winding number as one crosses the node. A Weyl node can only be gapped out by annihilation with a node of opposite chirality; hence such points are robust against small (and in 2D, symmetry-respecting) perturbations.

Previous work has demonstrated the construction of TNS analogues in bosonic systems such as photonic crystals [15]. The associated band touchings, however, occur at non-zero frequencies and the topological features are irrelevant when one is interested in only the low energy excitation of the system. Here we seek to construct a phonon analogue of TNS with protected zero-energy modes in the linearized phonon spectrum. These systems correspond to metamaterials or mechanical structures with robust extended soft modes which can be employed as building blocks of more complex structures requiring both rigidity for stability and flexibility for functionality [11, 12]. Fault tolerance, provided by topological protection, is highly desirable for applications in which different

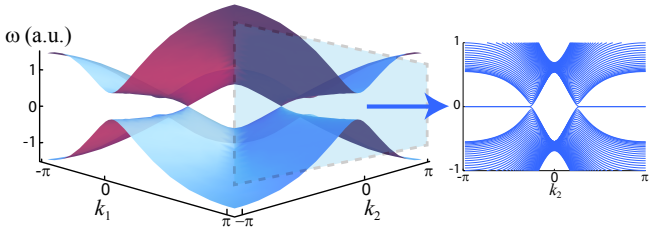

FIG. 1. Typical spectrum of a 2D TNS protected by chiral symmetry hosting a pair of topological nodes at $\omega = 0$ (only the two bands close to $\omega = 0$ are shown). The spectrum is computed for the fermionic problem defined in Eq. (2) with R defined in Eqs.(3) and (4). The parameters $(\theta_1, \phi_1, \theta_2, \phi_2) = (0.25, 0, 0.125, -0.125)\pi$ were used. The inset shows the edge spectrum when open and periodic boundary conditions are enforced for the $\hat{\boldsymbol{e}}_1$ and $\hat{\boldsymbol{e}}_2$ directions respectively, featuring a line of zero modes connecting the projections of the bulk topological nodes onto the surface Brillouin zone.

mechanical parts are coupled to perform non-trivial maneuvers. Similarly, our construction can also be applied to engineer acoustic or mechanical metamaterials with programmable response to external excitations [16, 17].

For a self-contained discussion, we first briefly describe phonon problems defined for mechanical structures formed by mass points connected by elastic elements modeled as central-force springs, and we review the boson-to-fermion mapping developed in Refs. [4–6]. The dynamics of such a system is determined by the kinetic energy of the mass points and the elastic potential energy stored in the springs, and therefore for N masses in d spatial dimension, a generic phonon problem can be defined by the Hamiltonian

$$\mathcal{H}_B = \sum_{\boldsymbol{r}} \left(\frac{\boldsymbol{p}_{\boldsymbol{r}}^2}{2m_{\boldsymbol{r}}} + \frac{1}{2} \sum_{j=1}^{z/2} \kappa_{\boldsymbol{r},j} s_{\boldsymbol{r},j}^2 \right), \tag{1}$$

where $\boldsymbol{r}$ denotes the equilibrium positions of masses $m_{\boldsymbol{r}}$, $\boldsymbol{p}$ denotes momentum of the masses, z is the coordination number, and $s_{\boldsymbol{r},j}$, $\kappa_{\boldsymbol{r},j}$ are respectively the extension and spring constant of the j-th spring. To simplify discussion, we set both $m_{\boldsymbol{r}}$ and $\kappa_{\boldsymbol{r},j}$ to unity for all $(\boldsymbol{r}, j)$ unless otherwise specified. Since we are interested in the existence of a bulk zero mode, we also impose periodic boundary conditions.

Generically, the spring extensions $\{s_{\boldsymbol{r},j}\}$ are functions of the displacements $\{\boldsymbol{x}_{\boldsymbol{r}}\}$ of the masses they connect. Within the harmonic approximation, the extensions are expanded to linear order in the mass displacements: $\boldsymbol{S} = R\boldsymbol{X} + \mathcal{O}(\boldsymbol{X}^2)$, where $\boldsymbol{X}$ is a dN dimensional column vector aggregating the displacement vectors of the N masses, and $\boldsymbol{S}$, similarly defined for the extensions $\{s_{\boldsymbol{r},j}\}$, is $zN/2$ dimensional. The $zN/2 \times dN$ dimensional matrix R is physically a linear map relating the spring extensions to the mass displacements. R^T is known as the equilibrium matrix and it relates the acceleration of the masses to the spring extensions: $\ddot{\boldsymbol{X}} = -R^T\boldsymbol{S}$. As in [6], henceforth we restrict attention to isostatic lattices, which have $z = 2d$ and so R is a square matrix. With this notation, the phonon Hamiltonian, within the harmonic approximation, can be recast as $\mathcal{H}_B = \frac{1}{2}\left[\boldsymbol{P}^2 + (R\boldsymbol{X})^2\right]$, where $\boldsymbol{P}$ is similarly defined as $\boldsymbol{X}$ and $R^TR = D$ is the real-space dynamical matrix. Equivalently, one can view R as a factorization of D.

The phonon modes are solutions to the eigenvalue problem $D\xi_i = R^TR\xi_i = \omega_i^2\xi$, where ω_i is the eigenfrequency of the i^{th} mode with $i = 1, \ldots, dN$. The bosonic phonon problem, characterized by R, can be mapped to a fermionic problem by considering a chiral matrix $\mathcal{H}_F$ and the associated Hamiltonian H_F [4–6]

$$\mathcal{H}_F = \begin{pmatrix} 0 & -iR^T \\ iR & 0 \end{pmatrix}; \; H_F = \begin{pmatrix} \bar{\boldsymbol{\chi}} & \boldsymbol{\chi} \end{pmatrix} \mathcal{H}_F \begin{pmatrix} \bar{\boldsymbol{\chi}} \\ \boldsymbol{\chi} \end{pmatrix}. \tag{2}$$

$\mathcal{H}_F$ satisfies $\{\tau^z, \mathcal{H}_F\} = 0$ with $\tau^z = \mathrm{diag}(1_{dN\times dN}, -1_{dN\times dN})$. One can easily verify the $2dN$ eigenvalues of $\mathcal{H}_F$ are given by $\{\pm\omega_i\}$, which implies the phonon spectrum is encoded in the energy spectrum of the fermionic Hamiltonian H_F. We note that only a subset of the zero modes of $\mathcal{H}_F$ give rise to zero modes of D; namely, those fermionic modes with $\tau^z = 1$. In contrast, fermionic zero-energy modes with $\tau^z = -1$ (i.e. null vectors of R^T) give rise to so-called states of self-stress of the mechanical problem [6]. $\boldsymbol{\chi}, \bar{\boldsymbol{\chi}}$ are Majorana fermions satisfying $\{\chi_l, \chi_m\} = \{\bar{\chi}_l, \bar{\chi}_m\} = \delta_{lm}$ with all other anti-commutators vanishing. In particular, χ ($\bar{\chi}$) is even (odd) under time reversal (TR). Since H_F corresponds to a TR symmetric Hamiltonian of spinless fermions, it belongs to the Altland-Zirnbauer symmetry class BDI [18].

Since the corresponding fermionic Hamiltonian is chiral, it can host topological nodes without fine-tuning even in 2D. To find a phonon analogue inheriting the topological features of the TNS, therefore, we consider the phonon spectrum arising from a spring-mass model defined on the square lattice ($d = 2$ and $z = 4$). For a regular phonon problem, the form of R is constrained by global translation invariance and point group symmetry of the underlying lattice. For the square lattice, one simply finds $\omega_j(\boldsymbol{k}) \propto |\sin k_j|$, where $j = 1, 2$ labels the two orthogonal directions. Although $\omega_j(k_j = 0) = 0$, these nodal lines are not topologically protected as they can be gapped out by breaking translation symmetry.

Here we relax from these symmetry constraints and assume they are explicitly broken. A possible realization is depicted in Fig. 2, in which the springs are tweaked with fixed, smooth pegs that serve as an external pinning potential. The form of R, however, is still constrained by the geometrical relations between the spring extensions and mass displacements. For a spring connecting the masses at $\boldsymbol{r}_a$ and $\boldsymbol{r}_b$, the spring extension should satisfy $|s| \leq |\boldsymbol{x}_{\boldsymbol{r}_a}| + |\boldsymbol{x}_{\boldsymbol{r}_b}|$. In particular, we assume that there is a

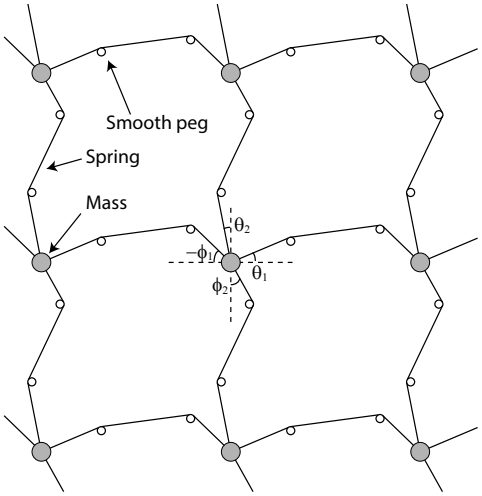

FIG. 2. A possible realization of the considered phonon problem. The dependence of the spring extensions on the displacements of the masses can be modified by bending the springs with fixed, smooth pegs that break global translation symmetry. The spring extensions are then characterized by Eq. (4) to linear order in mass displacements.

special spatial direction $\boldsymbol{v} = \cos\theta_a \hat{\boldsymbol{e}}_1 + \sin\theta_a \hat{\boldsymbol{e}}_2$ such that the inequality is saturated for $\boldsymbol{x}_{\boldsymbol{r}_a} = x_{\boldsymbol{r}_a}\boldsymbol{v}$ and $\boldsymbol{x}_{\boldsymbol{r}_b} = \boldsymbol{0}$. Equivalently, this implies we then have $\partial_{x_{\boldsymbol{r}_a,1}} s = \cos\theta_a$ and $\partial_{x_{\boldsymbol{r}_a,2}} s = \sin\theta_a$ in the original basis. Assuming a similar dependence of s on $\boldsymbol{x}_{\boldsymbol{r}_b}$, characterized by $\boldsymbol{w} = \cos\theta_b \hat{\boldsymbol{e}}_1 + \sin\theta_b \hat{\boldsymbol{e}}_2$, one finds $s = \boldsymbol{v}\cdot\boldsymbol{x}_{\boldsymbol{r}_a} + \boldsymbol{w}\cdot\boldsymbol{x}_{\boldsymbol{r}_b} + \mathcal{O}(\boldsymbol{x}^2)$.

For a clean system, all springs that are equivalent under lattice translation are characterized by the same parameters and in momentum space one finds

$$R(\boldsymbol{k}) = \begin{pmatrix} v_{11} + w_{11}e^{ik_1} & v_{12} + w_{12}e^{ik_1} \\ v_{21} + w_{21}e^{ik_2} & v_{22} + w_{22}e^{ik_2} \end{pmatrix}, \tag{3}$$

where $\boldsymbol{k} = (k_1, k_2)$ lies in the first Brillouin zone (BZ), and v_{lm} (w_{lm}) denotes the m-th component of the vector $\boldsymbol{v}_l$ ($\boldsymbol{w}_l$) relating spring extensions to the mass displacements $\boldsymbol{x}_{\boldsymbol{r}}$ and $\boldsymbol{x}_{\boldsymbol{r}+\hat{\boldsymbol{e}}_l}$. Enforcing the geometric constraints, the vectors can be parameterized by

$$\begin{aligned} \boldsymbol{v}_1 &= \begin{pmatrix} -\cos\theta_1 \\ -\sin\theta_1 \end{pmatrix};\ \boldsymbol{v}_2 = \begin{pmatrix} \sin\theta_2 \\ -\cos\theta_2 \end{pmatrix}; \\ \boldsymbol{w}_1 &= \begin{pmatrix} \cos\phi_1 \\ \sin\phi_1 \end{pmatrix};\ \boldsymbol{w}_2 = \begin{pmatrix} -\sin\phi_2 \\ \cos\phi_2 \end{pmatrix}. \end{aligned} \tag{4}$$

The sign convention of the angles are chosen to simplify subsequent expressions. The corresponding fermionic Hamiltonian, as defined in Eq. (2), is explicitly given by

$$H_F = 2i\sum_{\boldsymbol{r}}\sum_{l,m=1}^{2}\left(v_{lm}\chi^l_{\boldsymbol{r}}\bar{\chi}^m_{\boldsymbol{r}} + w_{lm}\chi^l_{\boldsymbol{r}}\bar{\chi}^m_{\boldsymbol{r}+\hat{\boldsymbol{e}}_l}\right). \tag{5}$$

Although the BDI class is topologically trivial in 2D, the system can inherit the non-trivial properties of the 1D system when identical 1D chains are stacked in one direction, similar to weak topological insulators. To this end, we introduce Fourier-transformed variables

$$\chi^l_{\boldsymbol{r}} = \frac{1}{\sqrt{N_2}}\sum_{k_2}\chi^l_{x_1,k_2}e^{-ik_2x_2};\ \chi^l_{x_1,k_2} = \frac{1}{\sqrt{N_2}}\sum_{x_2}\chi^l_{\boldsymbol{r}}e^{ik_2x_2}, \tag{6}$$

where N_j is the number of sites along the $\hat{\boldsymbol{e}}_j$ direction, and $\bar{\chi}^l_{x_1,k_2}$ is similarly defined. Since $(\chi^l_{x_1,k_2})^\dagger = \chi^l_{x_1,-k_2}$ is complex, one can define Majorana operators for $k_2 \in (0,\pi)$

$$\lambda_{x_1,|k_2|} = \frac{\chi^l_{x_1,k_2} + \chi^l_{x_1,-k_2}}{2};\quad \eta_{x_1,|k_2|} = \frac{\chi^l_{x_1,k_2} - \chi^l_{x_1,-k_2}}{2i}, \tag{7}$$

which are both even under TR. $\bar{\lambda}_{x_1,|k_2|}$ and $\bar{\eta}_{x_1,|k_2|}$, similarly defined for $\bar{\chi}_{x_1,k_2}$, are odd under TR. Since Eq.(5) only couples χ to $\bar{\chi}$, upon Fourier transform $H_F(k_2)$ will only couple (λ,η) to $(\bar{\lambda},\bar{\eta})$ and each such 1D system is in the BDI class. While the BDI class is classified by $\mathbb{Z}$ in 1D, the indexes of the 1D chains here are always even: the original lattice translational symmetry along $\hat{\boldsymbol{x}}_2$, reflected as a local $\mathcal{O}(2)$ rotation between $(\lambda_{x_1,|k_2|}, \eta_{x_1,|k_2|})$, guarantees that the Majorana zero modes at each edge occur in pairs. This can also be understood from the doubling of Majorana modes for each $k_2 \in (0,\pi)$, as $\chi^l_{x_1,k_2}$ and $\chi^l_{x_1,-k_2}$ are now Hermitian conjugates of each other. Such property of the system is more manifest by relabeling the operators as

$$c^A_{l,x,k_2} \equiv \chi^l_{x_1,k_2};\quad c^B_{l,x,k_2} \equiv \bar{\chi}^l_{x_1,k_2};\ k_2 \in (0,\pi) \tag{8}$$

such that c_l's are complex fermions. Eq.(5) is then decoupled into a series of 1D fermionic Hamiltonians, each labeled by $k_2 \in (0,\pi)$,

$$\begin{aligned} H_F(k_2) = 2\sum_x \Big[& iv_{11}c^{A\dagger}_{1,x}c^B_{1,x} + iv_{12}c^{A\dagger}_{1,x}c^B_{2,x} \\ & + iw_{11}c^{A\dagger}_{1,x}c^B_{1,x+1} + iw_{12}c^{A\dagger}_{1,x}c^B_{2,x+1} \\ & + i(v_{21} + w_{21}e^{-ik_2})c^{A\dagger}_{2,x}c^B_{1,x} \\ & + i(v_{22} + w_{22}e^{-ik_2})c^{A\dagger}_{2,x}c^B_{2,x} + h.c.\Big], \end{aligned} \tag{9}$$

where we have suppressed the subscript k_2 on the operators. The original chiral symmetry is manifested in this notation as a sublattice (A-B) symmetry.

To characterize these 1D systems, we further Fourier transform on x, which gives

$$H_F(k_2) = 2\sum_{k_1}\begin{pmatrix} \boldsymbol{c}^{A\dagger} & \boldsymbol{c}^{B\dagger} \end{pmatrix}\begin{pmatrix} 0 & iR_{-\boldsymbol{k}} \\ -iR^\dagger_{-\boldsymbol{k}} & 0 \end{pmatrix}\begin{pmatrix} \boldsymbol{c}^A \\ \boldsymbol{c}^B \end{pmatrix}, \tag{10}$$

where the subscript $\boldsymbol{k}$ of the operators is suppressed, $\boldsymbol{c}^A = (c_1^A, c_2^A)^T$, and similarly for $\boldsymbol{c}^B$. The bulk topological invariant of $\mathcal{H}_F(k_2)$ is given by the winding number of $\det(iR_{-\boldsymbol{k}})$ as k_1 is varied from $-\pi$ to π [7]. More explicitly, we have

$$\begin{aligned}\det(iR_{-\boldsymbol{k}}) =& -\left([\boldsymbol{v}_1 \wedge \boldsymbol{v}_2] + [\boldsymbol{v}_1 \wedge \boldsymbol{w}_2]e^{-ik_2}\right) \\ & -\left([\boldsymbol{w}_1 \wedge \boldsymbol{v}_2] + [\boldsymbol{w}_1 \wedge \boldsymbol{w}_2]e^{-ik_2}\right)e^{-ik_1} \\ \equiv & r_1(k_2) + r_2(k_2)e^{-ik_1},\end{aligned} \tag{11}$$

where $[\boldsymbol{v} \wedge \boldsymbol{w}]$ denotes the component of the wedge product $\boldsymbol{v} \wedge \boldsymbol{w}$ in the $\hat{\boldsymbol{e}}_1 \wedge \hat{\boldsymbol{e}}_2$ direction, and $r_1(k_2)$, $r_2(k_2)$ are introduced to simplify the expressions. The winding number $\mathcal{W}_{k_2}$ is determined by the relative magnitude of $|r_1(k_2)|$ and $|r_2(k_2)|$. The case of particular interest is when the winding numbers $\mathcal{W}_{k_2\to 0^+} \neq \mathcal{W}_{k_2\to\pi^-}$, which implies there must be a topological phase transition as k_2 is changed from 0 to π. Such a phase transition occurs when

$$\frac{|r_1(0)r_1(\pi)| + |r_2(0)r_2(\pi)|}{|r_1(0)r_2(\pi)| + |r_2(0)r_1(\pi)|} < 1, \tag{12}$$

and when this is satisfied the gap at $E = 0$ must close at some critical quasi-momentum $\boldsymbol{k}_c$, giving rise to a topological node. Such nodes in the fermionic picture are reflected in the original bosonic problem as a pair of isolated points $\pm\boldsymbol{k}_c$ at which the phonon frequency vanishes, corresponding to a bulk zero mode in the linearized spectrum.

For a system parameterized as in Eq. (4), we have

$$\begin{aligned}&\frac{|r_1(0)r_1(\pi)| + |r_2(0)r_2(\pi)|}{|r_1(0)r_2(\pi)| + |r_2(0)r_1(\pi)|} \\ =&\max\{|\cos(\theta_1 - \phi_1)|, |\cos(\theta_1 + \phi_1 - \theta_2 - \phi_2)|\},\end{aligned} \tag{13}$$

which implies that, for general parameters, its linearized phonon spectrum always contains a topologically protected bulk floppy mode. Note that if $\theta_1 + \phi_1 - \theta_2 - \phi_2$ is an integral multiple of π then ω accidentally vanishes on a pair of arcs in the BZ, rendering $\mathcal{H}_F(|k_2|)$ gapless for each $|k_2|$. For generic parameters, the critical quasi-momentum is

$$\boldsymbol{k}_c = (\theta_1 - \phi_1)\hat{\boldsymbol{x}} + (\theta_2 - \phi_2)\hat{\boldsymbol{y}}, \tag{14}$$

and therefore the quasi-momentum associated with the protected bulk floppy mode can be adjusted simply by tuning the angles θ_j and ϕ_j. Around $\pm\boldsymbol{k}_c$, the linearized phonon dispersion is conical and this forms an analogue of TNS (see supplementary material for details).

Since the two topological nodes located at $\pm\boldsymbol{k}_c \neq \boldsymbol{0}$ are isolated in momentum space, they are robust, in the fermionic picture, against small perturbations respecting chiral symmetry. This implies the phonon analogue is robust against weak arbitrary perturbations to the rigidity matrix, accommodating all the natural perturbations in a spring-mass model. Such robustness is demonstrated in the finite-size scaling shown in Fig. 3, in which we evaluate the disorder average of the lowest eigenfrequency found by numerically diagonalizing the linearized dynamical matrix. The sharp dips at $N = 20$ and 40 for $\sigma = 0$ are due to the matching between $\boldsymbol{k}_c$ and the finite-size sampling of the BZ. In the presence of disorder ($\sigma \neq 0$) the quasi-momentum ceases to be a good quantum number, but the bulk zero mode remains, as demonstrated by the decrease of $\langle\omega^2_{min}\rangle$ as system size increases.

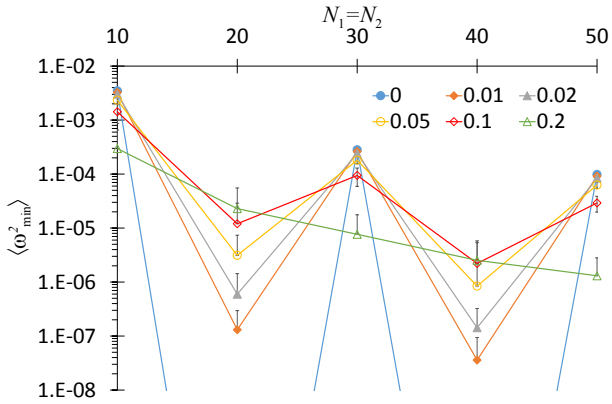

FIG. 3. Finite size scaling of the lowest eigenvalue of the disordered dynamical matrix. The linearized dynamical matrix for systems with size $N = N_1N_2$ and site-dependent couplings is numerically diagonalized to find the smallest eigenvalue $\omega^2_{\rm min}$. The clean system is defined by the set of physical parameters $\kappa = m = 1$ and $(\theta_1, \phi_1, \theta_2, \phi_2) = (0.1, 0.2, 0.2, 0.1)\pi$. Disorder is incorporated by adding to each parameter at each site a small, independent deviation drawn from a normal distribution with standard deviation σ. For each σ, the mean value $\langle\omega^2_{\rm min}\rangle$ is obtained from 200 disorder realizations. Error bars represent standard deviation in the disorder averages, and solid lines are guides for the eye.

Since the extended soft modes demonstrated here are protected by the topological properties of the linearized problem, one expects these modes to be only infinitesimal instead of finite. In addition, when the spring-mass system is only a model for a more general system, natural perturbations like the inclusion of small further neighbor couplings correspond to perturbations to the dynamical matrix instead of the rigidity matrix. Such perturbations can render the problem at hand non-isostatic and completely alter the structure of the analysis. The topological protection of the modes is generally lost when confronted with such perturbations, which will be the focus of future work. Therefore, we distinguish between the usefulness of this mapping when the bosonic problem is interpreted in a mechanical context (as done here), where local isostaticity is a binary question, as opposed to a quantum mechanical problem obtained after quantization, for which local isostaticity may only be an approximation.

In summary, we show that the mapping of bosonic phonon problems to chiral fermionic problems can be used to construct the phonon analogue of a topological nodal semimetal. In particular, we construct a 2D system that hosts a tunable bulk extended mode in its linearized phonon spectrum even when global translation symmetry is broken by an external pinning potential. Contrary to usual collective phonon modes arising from continuous symmetry breaking, the existence of such modes is not dictated by symmetry and has its roots in the topological properties of the corresponding fermionic problem. Such gapless topological bosonic modes are robust against disorder within the linearized description but are expected to be gapped when one performs a full phonon spectrum analysis. As long as the harmonic approximation is justified, the real phonon spectrum still contains such bulk soft modes at finite wavevector and they can be utilized to engineer metamaterials and mechanical structures with fault-tolerant properties.

Acknowledgment - We thank Haruki Watanabe for discussions. AV was supported by ARO MURI Grant W 911-12-0461. HCP appreciates financial support from the Hellman Fellows Fund; funding from NSF GRFP under Grant No. DGE 1106400 is also acknowledged (YB).

[1] S. Sachdev, *Quantum Phase Transitions*, Troisième Cycle de la Physique (Cambridge University Press, 2011), ISBN 9781139500210.
[2] X.-G. Wen, *Quantum field theory of many-body systems* (Oxford University Press, 2004).
[3] J. van Hemmen, Zeitschrift für Physik B Condensed Matter **38**, 271 (1980), ISSN 0722-3277.
[4] V. Gurarie and J. T. Chalker, Phys. Rev. Lett. **89**, 136801 (2002).
[5] V. Gurarie and J. T. Chalker, Phys. Rev. B **68**, 134207 (2003).
[6] C. L. Kane and T. C. Lubensky, Nat Phys **10**, 39 (2014), ISSN 1745-2473.
[7] M. Franz and L. Molenkamp, eds., *Topological Insulators*, vol. 6 of *Contemporary Concepts of Condensed Matter Science* (Elsevier, 2013).
[8] X. Wan, A. M. Turner, A. Vishwanath, and S. Y. Savrasov, Phys. Rev. B **83**, 205101 (2011).
[9] A. A. Burkov, M. D. Hook, and L. Balents, Phys. Rev. B **84**, 235126 (2011).
[10] V. Vitelli, N. Upadhyaya, and B. Gin-ge Chen, ArXiv e-prints (2014), 1407.2890.
[11] B. Gin-ge Chen, N. Upadhyaya, and V. Vitelli, ArXiv e-prints (2014), 1404.2263.
[12] J. Paulose, B. Gin-ge Chen, and V. Vitelli, ArXiv e-prints (2014), 1406.3323.
[13] K. Sun, A. Souslov, X. Mao, and T. C. Lubensky, Proceedings of the National Academy of Sciences **109**, 12369 (2012).
[14] O. Vafek and A. Vishwanath, Annual Review of Condensed Matter Physics **5**, 83 (2014).
[15] L. Lu, L. Fu, J. D. Joannopoulos, and M. Soljačić, Nature Photonics **7**, 294 (2013).
[16] R. Craster and S. Guenneau, *Acoustic Metamaterials: Negative Refraction, Imaging, Lensing and Cloaking*, Springer Series in Materials Science (Springer, 2012), ISBN 9789400748132.
[17] B. Florijn, C. Coulais, and M. van Hecke, ArXiv e-prints (2014), 1407.4273.
[18] A. Altland and M. R. Zirnbauer, Phys. Rev. B **55**, 1142 (1997).

SUPPLEMENTARY MATERIALS

Conical phonon dispersion for the smooth peg model

For a stable system, the phonon frequencies satisfy $\omega_\pm^2(\boldsymbol{k}) \geq 0$, where the $\pm$ sign corresponds to the two branches from diagonalizing the 2×2 dynamical matrix $D_{\boldsymbol{k}}$. As such $\omega_-^2(\boldsymbol{k})$ attains a global minimum at $\boldsymbol{k}_c$ and therefore $\boldsymbol{\nabla}_{\boldsymbol{k}}\omega_0|_{\boldsymbol{k}_c} = \boldsymbol{0}$. Expanding $\omega_-^2(\boldsymbol{k})$ around the nodal point $\boldsymbol{k}_c$, we have

$$\omega_-^2(\boldsymbol{k}_c + \delta\boldsymbol{k}) \approx \frac{1}{2}\sum_{ij} \frac{\partial^2(\omega_-^2)}{\partial k_i \partial k_j}\bigg|_{\boldsymbol{k}_c} \delta k_i \delta k_j. \tag{15}$$

The phonon speeds around the conical dispersion is given by:

$$\frac{1}{2}\left(\frac{\partial^2(\omega_-^2)}{\partial k_i \partial k_j}\right)\bigg|_{\boldsymbol{k}_c} = \frac{\kappa_1\kappa_2}{2(\kappa_1 s_1^2 + \kappa_2 s_2^2)} \begin{pmatrix} s_2^2 & s_1 s_2 c_\delta \\ s_1 s_2 c_\delta & s_1^2 \end{pmatrix} \tag{16}$$

where we let $s_j = \sin k_{cj}$ and $s_\delta = \sin\delta$ with $k_{cj} = \theta_j - \phi_j$ for $j = 1, 2$, and $\delta = \theta_1 + \phi_1 - \theta_2 - \phi_2$. The characteristic speeds around the nodal point is therefore given by

$$c_\pm^2 = \frac{\kappa_1\kappa_2(s_1^2 + s_2^2)}{4(\kappa_1 s_1^2 + \kappa_2 s_2^2)} \left(1 \pm \sqrt{1 - \left(\frac{2 s_1 s_2 s_\delta}{s_1^2 + s_2^2}\right)^2}\right) \tag{17}$$

where we let $s_\delta = \sin\delta$. It is clear that when $\delta = 0$, we have $c_- = 0$, corresponding to the softening of the phonon mode due to the line node; when $\delta = \pi/2$ and $s_1^2 = s_2^2$, we have $c_+ = c_-$ and this gives an isotropic conical dispersion.

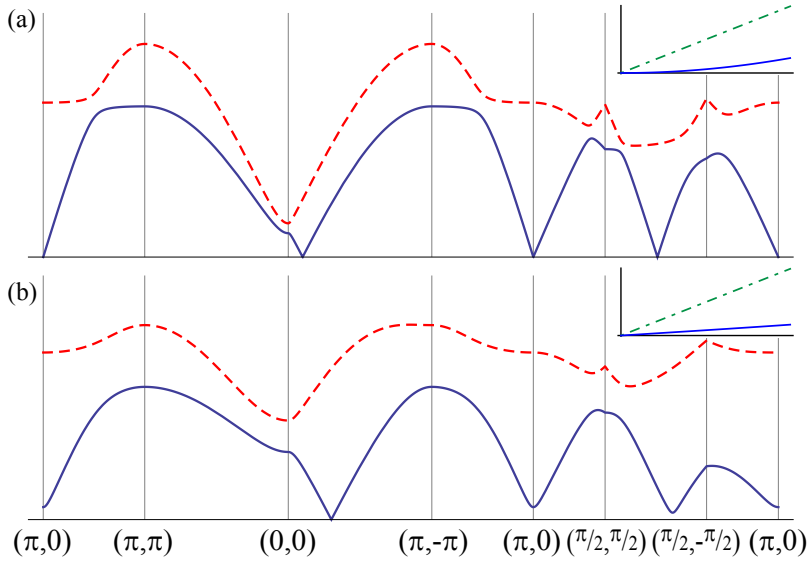

FIG. 4. Linearized phonon spectrum for the smooth peg model along different paths in the 2D BZ. The insets show the dispersion of the two independent phonon modes around the critical quasi-momentum $\boldsymbol{k}_c$. Here we take $m = \kappa_1 = 1$ and $\kappa_2 = 2$, which splits the partial degeneracy between the two phonon bands but does not affect the low energy dispersion. (a) The parameters $(\theta_1, \phi_1, \theta_2, \phi_2) = (.1, .2, .2, .1)\pi$ are used. The parameters satisfy $\theta_1 + \phi_1 - \theta_2 - \phi_2 = 0$, which gives rise to an accidental vanishing of ω along a pair of arcs in BZ. This is seen in the vanishing of ω at multiple values of $\boldsymbol{k}$ as well as the existence of a quadratic phonon mode around $\boldsymbol{k}_c$. (b) The parameters $(\theta_1, \phi_1, \theta_2, \phi_2) = (0.1, -0.2, -0.15, 0.15)\pi$ are used, which corresponds to the generic case in which the linaerized phonon spectrum contains a pair of isolated bulk nodal points at $\pm\boldsymbol{k}_c$ with conical dispersion around them.